Journal of Controlled Release 211 (2015) 74–84

Contents lists available at ScienceDirect

Journal of Controlled Release

journal homepage: www.elsevier.com/locate/jconrel

A systems approach to modeling drug release from polymer microspheres to accelerate *in vitro* to *in vivo* translation

Timothy D. Knab [a], Steven R. Little [a,b,c,e,f], Robert S. Parker [a,b,c,d,*]

[a] Department of Chemical and Petroleum Engineering, University of Pittsburgh, Pittsburgh, PA, USA
[b] McGowan Institute for Regenerative Medicine, University of Pittsburgh, Pittsburgh, PA, USA
[c] Department of Bioengineering, University of Pittsburgh, Pittsburgh, PA, USA
[d] Department of Critical Care Medicine, University of Pittsburgh, Pittsburgh, PA, USA
[e] Department of Immunology, University of Pittsburgh, Pittsburgh, PA, USA
[f] Department of Ophthalmology, University of Pittsburgh, Pittsburgh, PA, USA

ARTICLE INFO

Article history:
Received 28 October 2014
Received in revised form 28 February 2015
Accepted 11 April 2015
Available online 20 May 2015

Keywords:
Mathematical modeling
Reactive oxygen species
Adsorption
Controlled release
PLGA

ABSTRACT

Mathematical models of controlled release that span the *in vitro* to *in vivo* transition are needed to speed the development and translation of clinically-relevant controlled release drug delivery systems. Fully mechanistic approaches are often challenged due to the use of highly-parameterized mathematically complex structures to capture the release mechanism. The simultaneous scarcity of *in vivo* data to inform these models and parameters leads to a situation where overfitting to capture observed phenomena is common. A data-driven approach to model development for controlled drug release from polymeric microspheres is taken herein, where physiological mechanisms impacting controlled release are incorporated to capture observed changes between *in vitro* release profiles and *in vivo* device dynamics. The model is generalizable, using non-specific binding to capture drug–polymer interactions *via* charge and molecular structure, and it has the ability to describe both inhibited (slowed) and accelerated release resulting from electrostatic or steric interactions. Reactive oxygen species (ROS)-induced degradation of biodegradable polymers was incorporated *via* a reaction-diffusion formalism, and this suggests that ROS may be the primary effector of the oft-observed accelerated *in vivo* release of polymeric drug delivery systems. Model performance is assessed through comparisons between model predictions and controlled release of several drugs from various-sized microparticles *in vitro* and *in vivo*.

1. Introduction

There are currently a number of mathematical models that aim to explain the processes involved in drug release from biodegradable polymeric release systems. In general, these models work well to describe and predict release *in vitro*, and the most recent models are accurate for a wide variety of drugs and formulations. However, despite the successes in mathematically describing release *in vitro*, current models do not generally include drug–polymer interaction effects, and they often fail to accurately predict *in vivo* release. Phenomena such as drug–polymer interactions and the multitude of processes that may occur *in vivo* represent complex, poorly characterized systems. The inherent complexity of these phenomena makes the development of mechanistic mathematical models non-trivial; the sparsity of *in vivo* data further complicates modeling these processes.

In engineering, highly complex systems with many confounding variables abound. One method of approaching these problems is through systems engineering, where processes are conceptually simplified such that models capture key behaviors and dynamics of importance to the outcome, *e.g.*, drug release rate over time from a polymer drug delivery system. Systems-focused models forego mechanistic descriptions of highly interconnected and interdependent networks of processes in favor of a phenomenological description that captures key interactions and results in models that are easily employed in the design and control of processes, as the mathematical structure facilitates model incorporation into optimization and design algorithms. This approach is used herein to provide a generalizable characterization of drug–polymer interactions and to introduce a possible mathematical description of processes affecting *in vivo* drug release. Employing a systems engineering approach to capture these phenomena represents a shift in the mindset of controlled release modeling. The introduction of techniques to account for drug–polymer interactions and accurately capture *in vivo* release could dramatically reduce the cost and time required to develop controlled release formulations for clinical use by providing a method to accurately model drug–polymer systems in a wider range of environments.

* Corresponding author at: Department of Chemical and Petroleum Engineering, University of Pittsburgh, Pittsburgh, PA, USA.
E-mail addresses: tdk17@pitt.edu (T.D. Knab), srlittle@pitt.edu (S.R. Little), rparker@pitt.edu (R.S. Parker).

http://dx.doi.org/10.1016/j.jconrel.2015.04.045
0168-3659/

1.1. Background

Our group has previously developed a mathematical model that accurately predicts, in a regression-free way, the *in vitro* release profiles of a wide variety of clinically relevant drug–polymer combinations [1–3]. This model has been validated for a representative cross-section of biodegradable polymers including the most commonly used polyesters and polyanhydrides, particularly PLGA, yielding the most widely applicable predictive ability (to our knowledge) for a model to date. In its basic form the model will provide the foundation upon which we lay our phenomenologically motivated extensions. For the purpose of this analysis, we will choose a micro-spherical geometry, given its common usage in the field and the availability of *in vitro* and *in vivo* data.

1.1.1. Existing model framework

Electron micrographs of polymeric microspheres show pockets, or occlusions, within the particle matrix. Drug molecules trapped in these occlusions near the surface of the microspheres have a diffusivity dependent only on microsphere radius [4]. In general, this diffusivity is much greater than the drug diffusivity within the polymer matrix. As these pores open at the onset of microsphere hydration, the drug trapped within them is free to rapidly diffuse out of the particle resulting in the initial burst release. The subsequent lag phase results from the time required for the polymer to break down *via* hydrolysis, resulting in heterogeneous erosion and the maturation of the pore networks. Once the pore network develops to the point where a drug has a continuous pathway for diffusion to the surface, the lag phase concludes thereby leading to the second burst phase of release. Upon depletion of the encapsulated drug, the driving force for diffusion subsides and release terminates.

Functionally, this model is a realization of Fick's second law of diffusion in a spherical coordinate system with an evolving drug diffusivity [1–3]. Spatially, the diffusivity of the drug in the polymer matrix is piecewise discontinuous along the microsphere radius, r, with radial distance measured from the center of the particle. Any drug within one occlusion radius (R_{occ}) (the average diameter of a pore in the polymer matrix), of the surface initially experiences unhindered diffusion. Drug encapsulated within the particle beyond R_{occ} experiences a temporally evolving diffusivity (Eq. (1)) as water diffuses into the microsphere and begins to hydrolyze polymer bonds.

$$D_{eff}(t) = \begin{cases} D & \text{if } r > \left(R_{particle} - R_{occ}\right) \\ D\ \epsilon(MW(t)) & \text{if } r \le \left(R_{particle} - R_{occ}\right) \end{cases} \quad (1)$$

As the polymer matrix degrades and porosity ($\epsilon(MW(t))$) increases, the effective diffusivity of drug within the polymer matrix increases (Eq. (1)), asymptotically approaching the maximum diffusivity for any compound in a particle of that size [4]. It has been postulated that the amorphous regions of polymer degrade more rapidly than crystalline regions; as the amorphous regions degrade, they yield pores in a (comparatively) more crystalline polymer matrix [5–8]. The pore formation rate will follow a normal distribution if the following assumptions are made: (i) polymeric microparticles degrade heterogeneously; (ii) on average, a discrete pore has an equal probability of forming at any hydrated position in the polymer matrix; and (iii) polymer degradation rate is normally distributed. Because pore formation is a cumulative process, the matrix porosity as a function of polymer molecular weight will follow the cumulative normal distribution function, as follows [2]:

$$\epsilon(MW(t,r)) = 1 - \frac{1}{2}\left[1 + a\frac{erf(MW(t,r) - MW_r)}{\sigma\sqrt{2}}\right]. \quad (2)$$

The MW_r term in Eq. (2) represents the polymer molecular weight at which pores will have formed in the polymer matrix that are of suitable size to begin observing drug release. This delay in drug release while the polymer matrix degrades gives rise to the lag phase. Our previous work has correlated this to the molecular weight of the drug for common biodegradable systems [1]. Parameter σ in Eq. (2) is the standard deviation in polymer molecular weight at the time of pore formation, while parameter a in Eq. (2) adjusts the probability of finding a pore in the fastest degrading polymer of a polymer blend to match the probability of finding a region of polymer matrix that is purely amorphous. This ensures that the cumulative normal distribution results in pore formation in amorphous polymer, matching experimental observation [1].

Water diffuses into the polymer and reacts according to the reaction-diffusion scheme in Eq. (3) and the resulting polymer degradation is modeled by Eqs. (3) and (4). For small (~20 μm) microparticles, hydration is extremely rapid, with complete penetration occurring in a matter of minutes. However, hydration of larger microspheres is slowed due to an increased diffusion length and the greater potential for water to react with the polymer matrix before reaching the center of the particle. As the water diffusion front progresses through the microparticle the polymer matrix degrades with a first-order dependence on both the concentration of water and the molecular weight of the polymer matrix at that position. This leads to a spatiotemporally varying molecular weight profile throughout the microparticle as described by Eq. (4).

$$\frac{\partial[H_2O](t,r)}{\partial t} = D_{H_2O}\nabla^2[H_2O](t,r) - k_{deg}MW(t,r)[H_2O(t,r)] \quad (3)$$

$$\frac{\partial MW(t,r)}{\partial t} = -k_{deg}MW(t,r)[H_2O](t,r) \quad (4)$$

For copolymers, the degradation constant, k_{deg} in Eq. (4), is the sum of the degradation constants of the pure components, weighted by their fractional composition in the copolymer. Eqs. (1) to (4) describe the continuous diffusion of water into the microparticle and subsequent reaction with the polymer matrix resulting in a discontinuous and spatiotemporally evolving drug diffusivity. This unique varying drug diffusivity within the microparticle gives rise to burst-lag-burst phenomena often observed experimentally in release from biodegradable polymer matrices. Eqs. (1) to (4) are solved *via* the method of lines [9]. Briefly, the partial differential equation describing Fick's second law, Eq. (3), is spatially discretized into a set of ordinary differential equations using a finite difference method [9]; these equations, as well as the ordinary differential equation for polymer molecular weight degradation, are solved simultaneously *via* numerical integration with time as the independent variable. In the interest of computational simplicity, the microspheres are assumed to be spherically symmetrical (no variation in θ, ϕ) and discretization is required only in the radial direction. Under *in vitro* conditions, this model can capture the release behavior of a wide variety of drugs from polymeric matrices including degradable microspheres [1–3]. In the work presented here, the diffusion behavior of any additional molecules present in the polymer matrix, such as reactive oxygen species will be handled in the same way: the diffusion coefficient will be taken to be constant for small molecules with molecular weights on the same order as water, and larger releaseates will follow the previously derived molecular weight-based correlation (Eqs. (1) and (2)).

1.1.2. Tolterodine

Tolterodine is a muscarinic antagonist widely used to treat urinary incontinence. It is rapidly metabolized in the liver by cytochrome p450 to the active metabolite 5-hydroxymethyl derivative (DD01). DD01 exhibits similar pharmacokinetics as tolterodine, but interindividual variability in metabolic capacity results in very different ratios of tolterodine to DD01 in the plasma across patients. As a result, there is an interest in developing a controlled release formulation of tolterodine to reduce the variability in efficacy and decrease the occurrence of adverse side-effects in the patient population [10].

Tolterodine will be used as a case study for the engineering approach to modeling controlled release due to the availability of both *in vitro* and *in vivo* release data. In this case, tolterodine is encapsulated in 62.24 μm

50:50 RG503H poly(lactic-co-glycolic) acid (PLGA) microspheres and releases over approximately 30 days *in vitro* and 15 days *in vivo*. Using this case study and a systems engineering approach, we target the development of mathematical descriptors that explain tolterodine release both *in vitro* and *in vivo* and are extensible to the analysis of other agents and *in vivo* phenomena affecting the translation of *in vitro* to *in vivo* release. Tolterodine release data was obtained from a study performed by Sun et al. [10].

2. Methodology

2.1. Model development

Practical concerns drive the development of model extensions in this study. In general, models that explicitly and mechanistically account for known phenomena are desirable, but this is difficult to achieve in practice. For many systems, particularly in biology, the exact mechanisms and interactions of the participating components are poorly understood. Often coupled with a paucity of data, mechanistic models become difficult to identify, with the number of unknown or uncertain parameters leading to over-fitting of the scarce data. In response to these challenges, less complex phenomenological models are developed. The goal of these models is to describe data-driven observations in a manner that is consistent with fundamental theory and physics, without being directly derived from theory [11]. In following this philosophy for controlled release drug delivery, the goal is to increase the ability of our model to capture *in vivo* release for a wider range of compounds by utilizing available data to inform structural extensions to our model that employ a small number of additional fitted parameters. Doing so will result in a framework that can be used to identify trends in drug–polymer interactions and postulate *in vitro–in vivo* relationships for controlled release systems thereby aiding design and reducing development time and expense.

2.2. Parameter estimation

Model parameters were estimated using nonlinear least-squares regression as performed by *lsqnonlin* in MATLAB (©2014, the MathWorks, Natick, MA), with error measured as the difference between the simulated model output and experimental data. 95% confidence intervals were calculated using the *nlparci* routine included with MATLAB and are values reported after the ± for the fitted parameters.

3. Model extensions

3.1. Adsorption and desorption

In order to develop methods using *in vitro* data and experiments to inform models of *in vivo* release, it is crucial that the model first captures the *in vitro* system response. Comparing model predictions, with no extensions, to the tolterodine *in vitro* release data, the model predicts a release rate substantially faster than observed in the experiment (Fig. 1). This suggests that there must be an unaccounted-for mechanism that is working to significantly slow or inhibit tolterodine release from polymer microspheres. The interactions between tolterodine and PLGA are unknown, however potential interactions include phenomena such as electrostatics, sterics, or a combination thereof. It is known that many peptides and charged molecules physisorb to biodegradable polymers [12], so a simple and generic mechanism describing an adsorption-desorption equilibrium can be employed to capture a potentially more complex mechanism, as follows:

$$\frac{d[Drug_{ads}](t,r)}{dt} = k_{ads}\left[Drug_{free}\right]^{\omega}(t)\left(\frac{MW(t,r)}{MW_0}\right)^{\eta} - k_{des}[Drug_{ads}]^{\omega}(t,r)\left(1-\frac{MW(t,r)}{MW_0}\right)^{\eta} \tag{5}$$

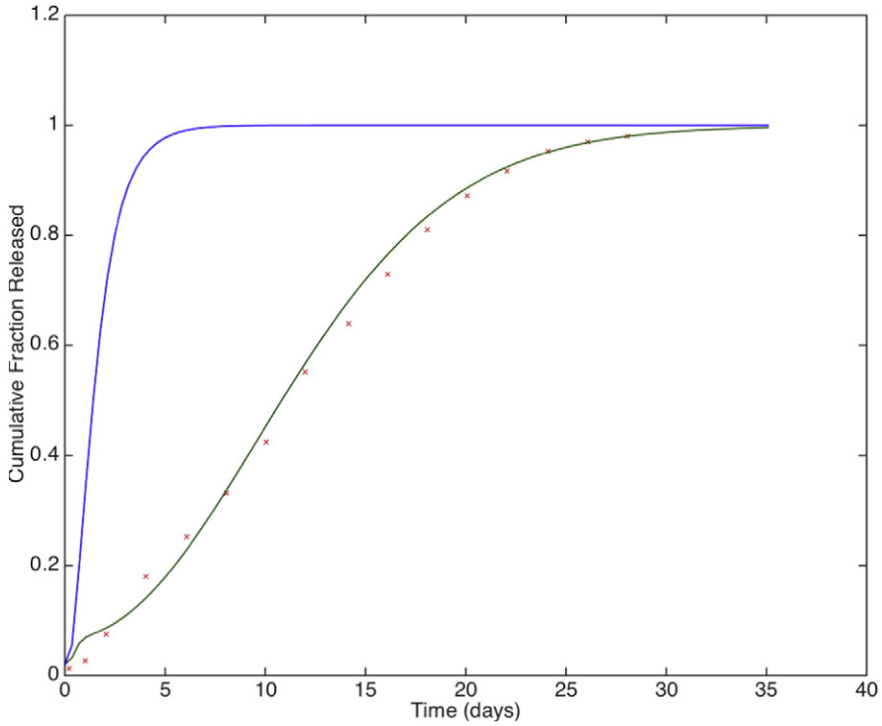

Fig. 1. Model predicted tolterodine release from 62.24 μm 50:50 RG503H PLGA microspheres compared to experiment (circles) [10] in the absence of drug adsorption-desorption kinetics (dashed line) and in the presence of adsorption-desorption kinetics (solid line) with optimal parameter values (± captures the parameter 95% CIs) $k_{ads} = 8.522 \pm 0.082$ $\frac{mol}{L \cdot s}$, $k_{des} = 1.416 \pm 0.020$ $\frac{mol}{L \cdot s}$, and $\omega = \eta = 1$.

$$\frac{d\left[Drug_{free}\right](t,r)}{dt} = D_{eff}\nabla^2\left[Drug_{free}\right](t,r) - k_{ads}\left[Drug_{free}\right]^{\omega}(t,r)\left(\frac{MW(t,r)}{MW_0}\right)^{\eta} + k_{des}[Drug_{ads}]^{\omega}(t,r)\left(1-\frac{MW(t,r)}{MW_0}\right)^{\eta}. \quad (6)$$

In this scheme, Eq. (5) describes the concentration of drug adsorbed to the polymer matrix as a function of the concentration of free, or unbound, drug, $Drug_{free}(t, r)$. Eq. (6) describes the concentration of free drug as it adsorbs and desorbs from the polymer matrix as well as diffuses out of the particle. The rate constant k_{ads} represents the rate of drug adsorption to the polymer matrix, and k_{des} represents the rate of drug desorption from the polymer matrix. Adsorption and desorption would be expected to depend on both the number of available sites on the polymer for the drug to adsorb, as well as the production of charged polymer ends as degradation progresses possibly resulting in drug–polymer electrostatic interactions. As such, both adsorption and desorption rates are postulated to be dependent on the polymer molecular weight. Note that the adsorption and desorption kinetics are not necessarily first order nor strictly integer-valued with respect to drug concentration or molecular weight. Exponent ω is treated as the number of drug molecules that can adsorb to η sites on the polymer matrix, where non-integer values can represent a single drug molecule requiring multiple polymer sites to bind. For strict adsorption-desorption interactions η is a positive exponent, representing a decrease in potential binding sites as the polymer degrades. In the case of electrostatic interactions the production of charged groups as a function of polymer degradation could result in stronger drug–polymer association resulting in a greater rate of adsorption and an equilibrium shift toward a higher degree of bound drug. This situation can be represented in this scheme through a negative value of η.

It is important to note that the addition of adsorption-desorption kinetics does not impact the model framework or alter the release mechanism postulated by the model framework (Section 1.1.1). Specifically the matrix porosity and drug diffusion (Eqs. (1) and (2)), are unaltered. Instead this adsorption-desorption mechanism decreases the rate of drug diffusion in the model framework.

The unknown parameters in Eqs. (5) and (6) (k_{ads}, k_{des}, ω, and η) were found *via* nonlinear least-squares regression. The result of this regression is shown in Fig. 1.

The values of the exponents ω and η were both estimated to be very close to 1 indicating first-order adsorption and desorption behavior with respect to both the concentration of drug and the molecular weight of the polymer matrix. This is the simplest possible case and indicates that we have posed a sufficiently flexible model structure that is both intuitive and effective. Fixing ω and η at 1 and re-fitting resulted in k_{ads} and k_{des} as reported in the caption of Fig. 1 with no significant loss in quality of fit. The unknown parameters in this adsorption–desorption framework are specific to drug–polymer combinations and should provide sufficient flexibility to capture a wide range of drug–polymer interactions based on *in vitro*.

3.2. In vivo degradation

Having developed a framework to account for drug–polymer interactions and estimated tolterodine-specific parameters, the differences between an *in vitro* and *in vivo* release environment need to be considered and reduced to a simple, generalizable mathematical description. It is often observed that release *in vivo* is significantly accelerated from *in vitro* experiments and correspondingly, *in silico* predictions of *in vitro* release [13–21]. The accelerated *in vivo* release of tolterodine is shown in Fig. 2.

This acceleration is hypothesized to be due to a more rapid breakdown of the polymer matrix *in vivo* stemming from an innate physiological response to a foreign body [22–28]. Specifically, biomaterial implantation produces tissue damage and disrupts endogenous cells and matrix leading to injury responses, such as mast cell degranulation and cytokine release. The release of cytokines drives a signaling cascade culminating in the localization of neutrophils and macrophages to the site of tissue injury. These cells have been implicated in the production of reactive oxygen species and are potentially responsible for the accelerated degradation of biodegradable polymers *in vivo*. [29–37], which would thereby increase the rate of drug release. A schematic of this process is presented in Fig. 3.

In a variety of *in vitro* studies, it is observed that inflammatory cells produce reactive oxygen species (ROS) in response to biomaterials [33–36]. Biomaterials implanted in mice have been shown to generate a similar production of reactive oxygen species *in vivo* [39]. These ROS include molecules such as superoxide (O_2^-), hypochlorite ($ClO-$), hydrogen peroxide (H_2O_2), and the hydroxyl radical (OH) and all have been shown to have degradative capacity for biomaterials, specifically toward poly(D,L-lactic) acid [40,41] and polyurethanes [42]. The current body of literature points to ROS as a highly likely mediator of the commonly observed accelerated *in vivo* degradation phenomenon. To our knowledge, a phenomenological mathematical description of polymer degradation by ROS has yet to be developed.

3.2.1. Reactive oxygen-mediated degradation

Reactive oxygen species-mediated ester bond breakage is thought to proceed *via* a free radical chain reaction mechanism, the kinetics of which are currently not well understood. As such, a mass action rate law is postulated such that the overall degradation of the polymer network has a contribution from both hydrolysis and ROS (Eq. (7)):

$$\frac{dMW(t,r)}{dt} = -kMW(t,r)[H_2O](t,r) - k_{ROS,MW}MW^{\alpha}(t,r)[ROS]^{\beta}(t,r). \quad (7)$$

The exponents α and β represent the reaction orders for the ROS-mediated degradation of the polymer matrix with respect to the polymer molecular weight and ROS concentration within the polymer matrix at a given position and time. The concentration of reactive oxygen species within the polymer matrix is given by the partial differential equation (PDE) Eq. (8) where D_{ROS}, the diffusion coefficient of the ROS in the polymer matrix, is taken to be a constant due to the small size of reactive oxygen species and their rapid diffusion within the polymer matrix independent of porosity. The concentration of ROS is tracked spatially within the polymer matrix through Eq. (8), necessitating the solution of Eq. (7) at every spatial discretization point within the polymer matrix.

$$\frac{\partial[ROS](t,r)}{\partial t} = D_{ROS}\nabla^2[ROS](t,r) - k_{ROS}MW^{\gamma}(t,r)[ROS]^{\lambda}(t,r) \quad (8)$$

It is important to note that Eq. (8) contains different rate constants and reaction orders than Eq. (7). This is because other reactive intermediates may be generated during the propagation steps, under the assumption of a chain reaction mechanism. Thus, the rate of polymer degradation by ROS is not necessarily the same as reactive species consumption, and the orders of the reactions that consume and generate reactive species may be different. In this scheme, k_{ROS} may take on negative values if the rate of reactive species generation during the propagation steps is greater than the rate of reactive species consumption in the chain termination steps.

The framework developed here describes the possible degradation of polyester biomaterials by radical species and follows established chemical principles without explicitly describing what could otherwise be a very complicated chain reaction mechanism with many rate parameters to identify without explicit data to elucidate the individual steps of the mechanism of degradation.

3.2.2. ROS parameter estimation

To estimate values for the parameters governing ROS-mediated biomaterial degradation kinetics, Eq. (7) was regressed to experimental

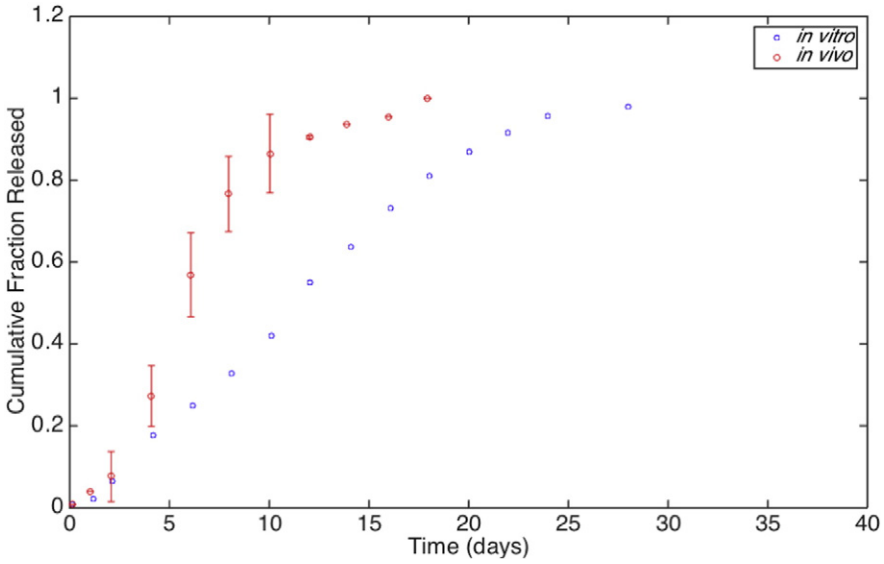

Fig. 2. Tolterodine release from approximately 60 μm RG503H (50:50 PLGA, MW = 28,000) at 37 °C [10].

data taken from Lee et al. (1999) [43]. The diffusion and chain reaction of reactive species (Eq. (8)) was not considered, as this experiment was carried out in a polymer solution, not a polymeric matrix. It is important to note that this experiment was performed in tetrahydrofuran (THF) and thus the water hydrolysis of PLA can be ignored. Furthermore, the fact that this experiment was undertaken in THF means that the rapid superoxide dismutation reaction in water to form peroxides can be ignored and the superoxide can be assumed to be constant. As a result of the experimental conditions, fortuitously, the resultant parameters are specific only to the superoxide hydrolysis of PLA and the regression is not a function of the water hydrolysis reaction. In this regression, the matrix molecular weight after 24 h was fitted over a range of superoxide concentrations. Fitted parameters were the reaction rate, (k_{ROS}), and partial reaction orders for both the polymer molecular weight and the reactive oxygen species concentration (α and β, respectively, in Eq. (7)). In doing this we are taking the molecular weight to be analogous to the concentration of ester bonds in the biodegradable polyester and the reactive oxygen species is superoxide.

Reaction orders α and β were not constrained to integer values, as is usually seen in rate laws. Fractional reaction orders are often used to capture chain reaction-type mechanisms—consistent with possible free radical ROS-induced reactions in the polymer network [44,45]. The results of our regressed kinetics, compared to the experimental data, are shown in Fig. 4. Orders α and β can be rounded to 3.5 and 2, respectively, with no significant loss in quality of fit; these parameters are taken to be constant at these values throughout the remainder of this study.

Under the assumption that this rate law is general for an array of physiologically relevant reactive oxygen species, the mechanism was verified using another literature data set [40] where the degradation of PLA pellets in the presence of hydroxyl radicals generated through a Fenton reaction was studied. This study collected data over 30 weeks, and even then did not observe total degradation of the pellets in an aqueous environment. Because PLA degradation proceeds *via* hydrolysis, water needs to fully hydrate the particle to observe complete degradation. The observed, lengthy degradation suggests large pellets degrading *via* a surface erosion mechanism, as water is consumed by reaction near the surface of the particle leaving little water to diffuse throughout the extent of the particle. Accounting for the diffusion of water into the pellet (Eq. (3)), hydrolytic degradation kinetics only (Eq. (4)), and fitting the radius of a spherical pellet that would be consistent with the experimental data returned a value of 0.81 mm. This result is consistent with the critical lengths established by Burkersroda et al. [46]. Failure to account for the diffusion of water into the pellet, using instead the assumption of rapid hydration, results in a degradation rate–by hydrolysis alone–that far exceeds the experimentally observed rate of molecular weight loss.

As OH is small in size (comparable to water), pore formation was assumed to be irrelevant to ROS transport, and OH diffusivity (D_{ROS} in Eq. (8)) was assumed to be the diffusivity of OH in an aqueous environment ($1.3 \times 10^{-4}\ \frac{m^2}{day}$) [44]. The concentration of OH in the aqueous environment, which is used as the boundary condition at the surface of the particle ($ROS_{aqueous}$ in Table 1), was unknown and fitted *via* nonlinear

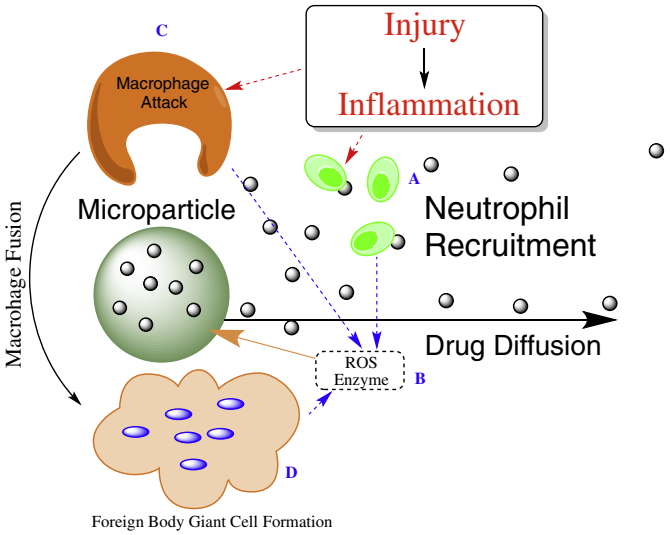

Fig. 3. A chemokine gradient established by injured cells and tissue exudate results in neutrophil recruitment to the site of implantation (A). In response, neutrophils release reactive oxygen species (ROS), degradative enzymes, and key signaling molecules (IL-4 and IL-14) (B) [32]. Continued presence of the foreign body leads to macrophage recruitment. Macrophage will attempt to phagocytose the biomaterial (C), but in cases where the implanted device is too large (>~10 μm), macrophage may undergo fusion to form large multinucleated cells referred to as foreign body giant cells (FBGCs) (D). This process of macrophage fusion is a hallmark of the foreign body response [38].

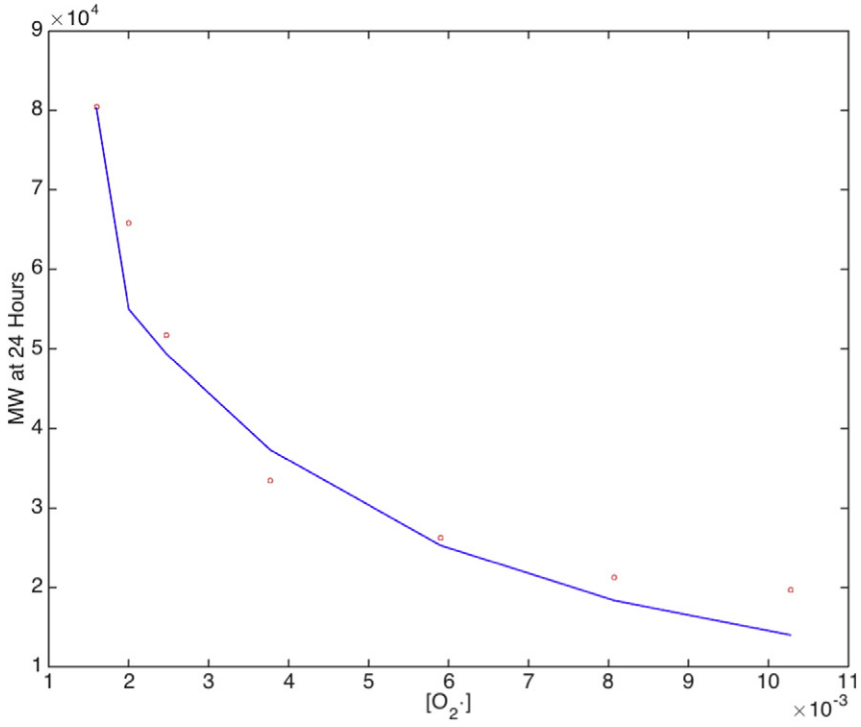

Fig. 4. Molecular weight of Polylactic Acid (PLA) in the presence of varying superoxide concentrations. Circles are experimental data, Solid line is model fit. $k_{ROS,MW} = 6.328 \times 10^{-6} \pm 8.74 \times 10^{-6}$ $\frac{L^2}{Da^{2.5}Mol^2 \cdot s}$, $\alpha = 3.5 \pm 0.523$, $\beta = 2 \pm 1.039$.

regression. Under the assumption that the mechanism is the same as for superoxide, the reaction orders, α and β, were taken to be 3.5 and 2, respectively, as previously determined. In addition to regression of the diffusion parameters, it is necessary to fit k_{ROS}, the rate of ROS consumption or generation, as well as γ and λ, the reaction orders for the consumption or generation of ROS as the chain reaction mechanism breaks down the polymer matrix within the microspheres. The initial regression resulted in reaction orders γ and λ that were approximately 1. Rounding these values to exactly 1, implying first order reactions in both ROS and the polymer matrix (*MW*), and then regressing the remaining parameters simplified the model without significantly impacting quality of fit. The fitted results are shown in Fig. 5 and Table 1.

As previously noted, OH is generally more reactive than superoxide, and as expected the rate of PLA degradation in the presence of hydroxyl radical is higher than with superoxide.

3.3. In vivo release

Returning to the tolterodine case study, the proposed adsorption–desorption kinetics (Section 3.1) were applied simultaneously with the postulated reactive oxygen-mediated polymer degradation kinetics (Section 3.2.1) to the model framework and nonlinear least-squares regression was used to fit simultaneously the *in vitro* and *in vivo* data with a common parameter set. Notably, the tolterodine microspheres being studied here are synthesized from the biodegradable polyester poly(lactic-co-glycolic) acid (PLGA), not PLA as in ROS.

Table 1
Parameter values for hydroxyl radical degradation of spherical 0.81 mm PLA pellets.

Parameter	Value	Units
$k_{ROS,MW}$	0.037	$\frac{L^{2.4033}}{Da^{1.4320}Mol^{0.4033} \cdot s}$
k_{ROS}	2.16	$\frac{L}{Mol \cdot s}$
D_{O_2}	2.02×10^{-4}	$\frac{m^2}{day}$
$[ROS_{aqueous}]$	1.11×10^{-4}	$\frac{Mol}{L}$

We postulate that the different chemical structures between PLA and PLGA will require changes to parameters describing the rate of degradation, but there is no reason to consider different mechanisms of degradation for such closely related polymers. As such α and β were fixed at 3.5 and 2 respectively, as determined in ROS. Similarly γ and λ were fixed at 1. ω and η were also fixed at 1, as determined in Section 3.1. A summary of parameters and their origins is shown in Table 2. The model simulation after fitting is shown in Fig. 6.

4. Discussion

As expected, the rate constant for the ROS-mediated degradation of PGA is higher than that of PLA, and the diffusion of the ROS is similar in magnitude to water. Additionally, the rate of ROS consumption within the microsphere is less than observed in the PLA-hydroxide case (ROS), which is encouraging, as we would expect the *in vivo* ROS environment to be a combination of many potential radicals, with the hydroxyl radical being the most reactive and thus representing an upper bound for the rate of ROS consumption. Furthermore, the ROS concentration exterior to the particle is well within the physiological range (<~150 μM). With the ability of the resulting model to capture literature data, the phenomenological descriptions employed for binding and ROS-mediated degradation, in tandem with mass-action kinetics, provide a structure that describes both *in vitro* and *in vivo* drug release.

The top panel of Fig. 6 (the *in vivo* fit) shows an overprediction of release over the first few time points, this is because our model was designed to capture the *in vitro* magnitude, but not the dynamics, of the burst release from the polymer microspheres. As a result there is a clear discrepancy *in vivo* over the first few hours of release.

Further validation was undertaken using *in vitro* and *in vivo* data for Huperzine A release from formulation F taken from Chu et al. [14]. In this validation k_{ROS}, and $k_{ROS,MW_{PGA}}$ were taken to as the results from the tolterodine regression as 50:50 RG503H PLGA was also used in this formulation as these parameters should span all 50:50 RG503H PLGA microparticles. Regressed parameters were k_{ads}, k_{des}, η, ω, which

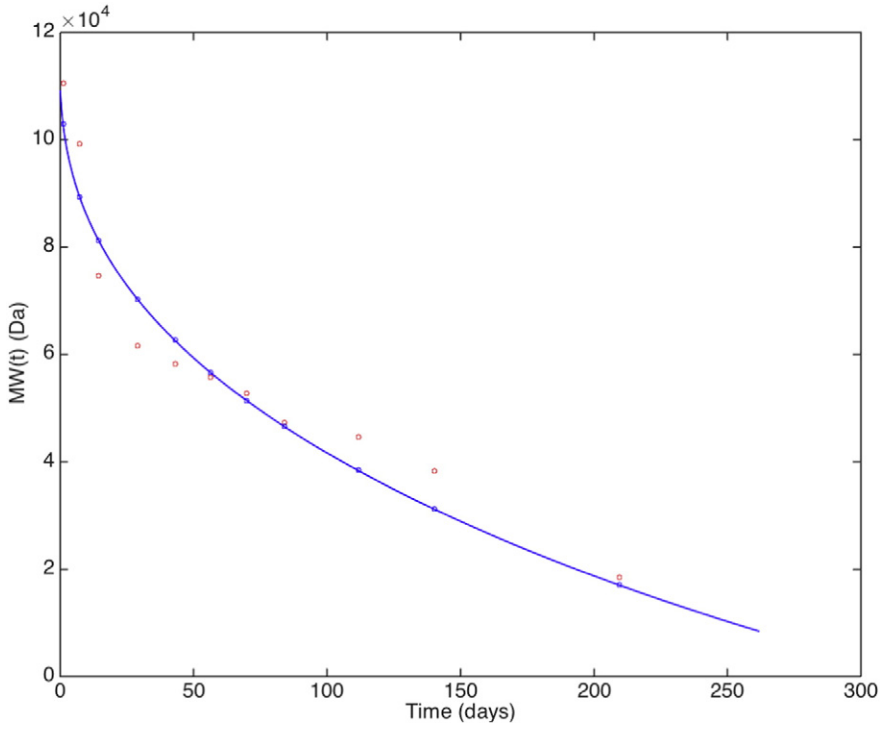

Fig. 5. Molecular weight of spherical (R = 0.81 mm) Polylactic Acid (PLA) pellets in the presence of hydroxyl radical. Circles are experimental data, solid line is model fit with ROS kinetics [40].

are all specific to a particular drug–polymer combination, as well as [$ROS_{aqueous}$]. The results and parameter values from this regression are shown in Fig. 7 and Table 3, respectively.

As is evident from Fig. 7 we again obtain a very good agreement between our proposed model and both *in vitro* and *in vivo* data by fitting only a few coefficients. Further support for model extensibility comes in the external concentration of ROS, which was regressed in the validation as similar to that previously calculated when fitting the tolterodine data. This is notable as it implies that a common set of ROS parameters for a given polymer may be able to be used to describe many different drugs using only drug-specific parameters.

From Fig. 7 we see that the Huperzine A microparticles do not exhibit a substantial burst release and the model accurately captures experimental release data across the entire time course, both *in vitro* and *in vivo*. This provides further evidence that the discrepancy in burst model predicted burst release in Fig. 6 is due to undermodeling of burst release dynamics.

Table 2
Parameter values for simultaneous fitting of *in vivo* and *in vitro* Tolterodine data.

Parameter	Units	Origin	Value ± 95% confidence interval
α	–	Fitted in Section 3.2.2	3.5 ± 0.523
β	–	Fitted in Section 3.2.2	2 ± 1.0389
k_{ROS}	$\frac{L}{Mol\,s}$	Fitted in Section 3.3	0.52099 ± 0.00374
$k_{ROS,MW_{PLA}}$	$\frac{L^2}{Da^{2.5}Mol^2\,s}$	Fitted in Section 3.2.2	$6.328 \times 10^{-6} \pm 8.74 \times 10^{-6}$
$k_{ROS,MW_{PGA}}$	$\frac{L^{2.4033}}{Da^{1.4320}Mol^{0.4033}\,s}$	Fitted in Section 3.3	0.050 ± 0.0316
D_{O_2}	$\frac{m^2}{day}$	Section 3.2.2 (Literature)	1.3×10^{-4}
γ	–	Section 3.2.2	1
λ	–	Section 3.2.2	1
[$ROS_{aqueous}$]	$\frac{Mol}{L}$	Fitted in Section 3.3	$1.27 \times 10^{-4} \pm 8.54 \times 10^{-5}$
k_{ads}	$\frac{Mol}{L\,s}$	Fitted in Section 3.1	8.522 ± 0.0822
k_{des}	$\frac{Mol}{L\,s}$	Fitted in Section 3.1	1.416 ± 0.0204
ω	–	Section 3.1	1
η	–	Section 3.1	1

4.1. Other possible accelerated degradation mechanisms

We have postulated that reactive oxygen species (ROS)-mediated degradation of the polymer matrix is responsible for accelerated *in vivo* degradation and drug release, however it is known that certain enzymes such as lipases, lysozymes and esterases exhibit biodegradative activity toward biodegradable polymers [45,31,46,47,30,32,29,48,49]. Here we employ our model to study the potential effects of enzymatic degradation under the assumption that degradative enzymes would have the same transportation kinetics and correlations [1] governing their diffusion into a microparticle as drug releasing from the microparticle. As such, an enzyme with a molecular weight in the tens of kDa (same order of magnitude as lysozyme, lipases *etc.*) would have a near zero diffusion coefficient within the polymer matrix until the polymer matrix reached a molecular weight well below 1000 Da. In our experience, the microparticles begin to break apart at approximately 1500 Da. Hence, we postulate that enzymes are unable to provide the breakdown observed throughout the microparticles over the course of degradation.

To test the above hypothesis *in silico*, we explored the possibility that enzymes may account for accelerated *in vivo* degradation in our model. The extent of potential accelerated enzymatic degradation was studied by allowing a "generic" enzyme with a molecular weight similar to that of human lysozyme to diffuse from the particle surface into the bulk of the microparticle following (Eqs. (1) and (2)). The enzyme was assumed to degrade the polymer matrix according to a pseudo-Michaelis–Menten rate expression (Eq. (9)) where [S], the substrate concentration is taken to be analogous to molecular weight of the polymer matrix. A model drug with a MW_r of 4.8×10^3 Da was chosen to compare release between degradation by hydrolysis only and degradation by pure hydrolysis and enzyme-catalyzed hydrolysis.

$$\nu = \frac{V_{max}[S][E]}{K_m + [S]} \tag{9}$$

Assigning our model enzyme a V_{max} and K_m corresponding to a turnover number 600,000 s^{-1} (faster than carbonic anhydrase, one of the

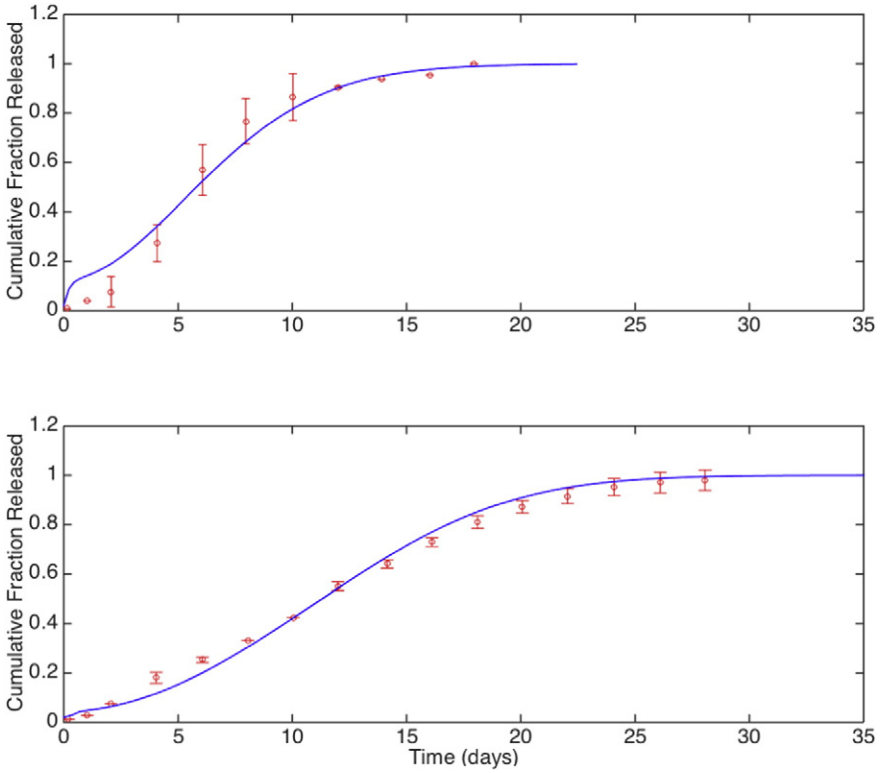

Fig. 6. Model predicted tolterodine release (solid line) from 62.24 μm 50:50 RG503H PLGA microspheres compared to experiment (circles). (Top) *in vivo* fit (bottom) *in vitro* fit.

fastest enzymes [50]) and an efficiency $>10^{10}\,M^{-1}\,s^{-1}$ (greater than superefficient enzymes such as fumarase [51]), respectively resulted in the molecular weight profiles shown in Fig. 8.

From Fig. 8 we see that the enzyme, despite having an activity and efficiency toward the degradation of PLGA higher than any currently known activities and efficiencies results in cumulative fraction of drug released that is at most, less than 1% greater than non-enzyme mediated degradation. This is due to the fact that the large size of enzymes restrict them to surface erosion and although they clearly alter the spatio-temporal molecular weight profile within the microparticle as seen in the top panel of Fig. 8 they do not have a significant effect on release.

In general, the concentration of drug within the microparticle will be depleted and release will cease before a potentially degradative enzyme has eroded and diffused into a significant bulk of the microparticle. Even

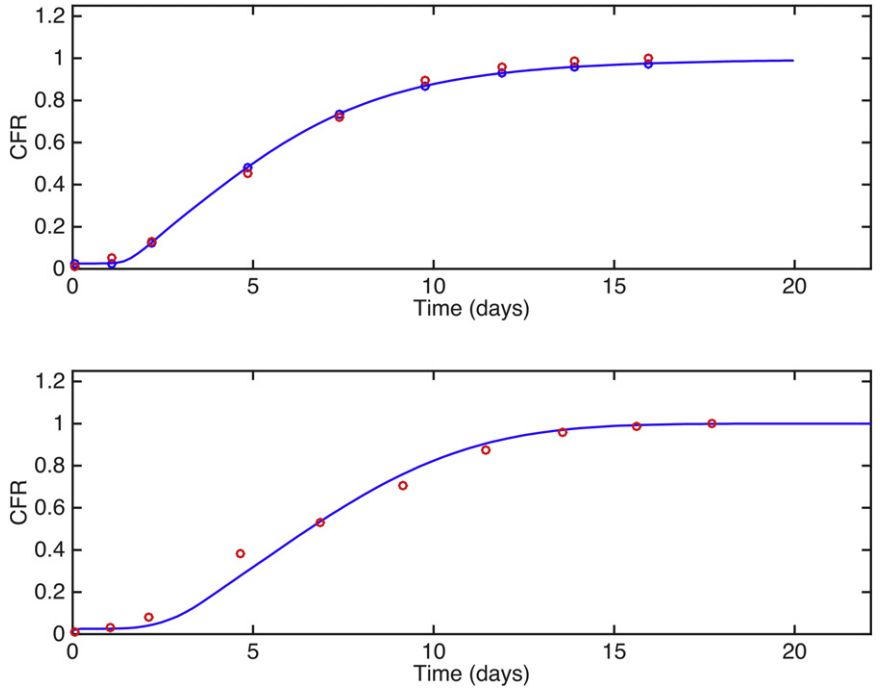

Fig. 7. Model predicted Huperzine A release (solid line) from 113.2 μm 50:50 RG503H PLGA microspheres compared to experiment (circles). (Top) *in vivo* fit (Bottom) *in vitro* fit.

Table 3
Parameter values for simultaneous fitting of *in vivo* and *in vitro* Huperzine A data.

Parameter	Value	Units
k_{ads}	2.354	$\frac{1}{\text{Mol}^{0.72}\ \text{s}}$
k_{dex}	0.820	$\frac{1}{\text{Mol}^{0.72}\ \text{s}}$
η	1.72	–
ω	1.988	–
$[ROS_{aqueous}]$	7.2495×10^{-5}	$\frac{\text{Mol}}{\text{L}}$

for large drugs (on the same order of magnitude as potential degradative enzymes) drug release requires near total microparticle dissolution thus nullifying any enzymatic effects. In addition to our modeling results, a number of studies [52–55] have refuted the claim that enzymatic degradation is responsible for accelerated *in vivo* drug release from biodegradable polyesters.

Through phenomenological modeling and regression of a minimal common parameter set we believe we can implicate reactive oxygen species-mediated degradation in observed accelerated degradation of polymer matrices and drug release *in vivo*.

Furthermore, we would expect to see slowed *in vivo* release kinetics through suppression of ROS *via* antioxidants or other means. In fact, a number of studies [56,42,57,5] have shown decreased *in vivo* degradation of biodegradable polymers through the delivery of antioxidants to the local implant site. This particular study set has not been replicated herein due to the need to retrospectively fit the ROS suppression kinetics as a function of antioxidant concentration and reactivity with ROS. Instead, we note the original model neglects ROS-mediated degradation and demonstrates slower degradation kinetics, thereby implying that the postulated model has the fidelity to capture a slowing of ROS-mediated degradation.

In summary, we have put forth a mechanism that recapitulates the characteristics expected of ROS effects on *in vivo* release but does not exhibit the properties that would be expected of accelerated degradation due to other mediators, thereby strengthening the implication of ROS-mediated degradation.

4.2. Further considerations

A drawback of this regression approach is that the objective function surface for the adsorption-desorption kinetics contains many local minima, and as such these parameters need to be fit simultaneously to both the *in vitro* and *in vivo* data sets. Applying the parameters obtained from fitting the adsorption-desorption kinetics to the *in vitro* data alone locates the model in a region of parameter space where the *in vivo* data cannot be quantitatively fit if ROS concentrations are limited to the physiologic range. In addition, the *in vivo* fit assumes a constant external concentration of ROS at or below the physiologic limit. In an *in vivo* situation, these concentrations would be dynamic, and onset of ROS production would likely be delayed somewhat from biomaterial implantation. This has not been implemented due to both the lack of data and a model for local ROS concentrations following implantation. Fitting the model parameters in the presence of dynamic ROS concentrations could provide increased confidence in the parameter values, and potentially a better match to dynamic drug release data if the physiological response demonstrates significant changes in local tissue response to biomaterial implantation. These are avenues of potential further study, and could provide better limits on parameter values for the model.

Despite these shortcomings, we have developed a model that accounts for the effects of a very complicated cascade of biological responses on drug delivery from controlled release polymer systems. Furthermore, this framework is able to accurately match experimentally observed *in vivo* release data utilizing ROS-mediated degradation. This suggests that ROS is a primary mediator of accelerated *in vivo* release.

A major advantage of the approach discussed herein is that it is able to implicate a specific mechanism and explore how said mechanism impacts release behavior, which is characteristically different from an *in vitro–in vivo* correlation (IVIVC), which simply maps an *in vitro* release rate to an *in vivo* one with no predictive power or extensibility to other drug–polymer combinations. Furthermore, our model responds to differences in conditions *in vitro* and *in vivo*, where the IVIVC is for specific *in vitro* condition sand is much less robust to interpatient variability and *in vivo* changes that may occur.

Although there may be other physiologic mechanisms at play *in vivo*, we believe that the ability of our model to capture release data using a comparatively simple mathematical formulation indicates the high importance of ROS to the overall release process. Following a systems engineering rationale, it can be argued that the contributions of other effects not explicitly included are effectively and implicitly accounted for in fitting the model parameters.

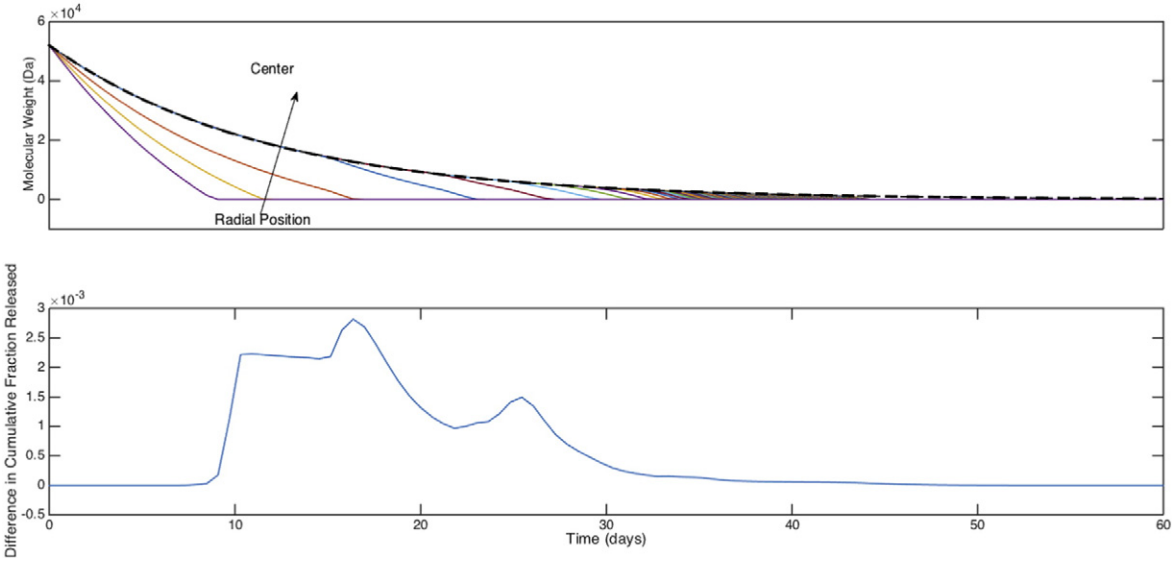

Fig. 8. (Top) Molecular weight of 20 μm microparticle degrading in the presence of hypothetical extremely active enzyme. Dashed line indicates degradation without enzyme. (Bottom) Release profile of particle degrading in the absence of the enzyme subtracted from the release profile of a particle degrading in the presence of an enzyme.

5. Summary

Utilizing a systems engineering philosophy, we have developed extensions to our existing controlled release model to extend applicability to a wider range of drugs and to include *in vivo* release. Incorporating the adsorption–desorption mechanism improves *in vitro* model predictions of drug release for certain drug–polymer combinations where interactions between the two are likely occurring. We ascribe the oft-observed *in vivo* acceleration of release (compared to *in vitro*) to the generation of reactive oxygen species, which are produced through an innate foreign-body response *in vivo*. A postulated model of ROS-mediated biomaterial degradation was shown to be consistent with literature data and combined with the adsorption-desorption model a framework that can accurately describe the release of tolterodine and Huperzine A from PLGA microspheres *in vivo*. The model extensions developed herein contain a limited number of parameters that need to be regressed to experimental data, thereby avoiding the potential for overfitting that could occur with a mechanistically-oriented model. From these case studies, we believe that drug release from polymeric microspheres *in vivo* can be accurately described by our model that: (i) postulates kinetics of ROS-mediated polyester degradation that are valid for a variety of experimental data from the literature; and (ii) incorporates these ROS-mediated kinetics within a previously developed and validated mathematical framework. Finally, the model could be used in a design context to speed the time required to reach clinical testing of polymeric drug delivery formulations in that it would allow *in vitro* results to drive *in vivo* experiment with a higher degree of confidence than currently achievable.

Acknowledgments

This work was supported by the U.S. Department of Education through the GAANN awards P200A100087 and P200A120195.

SRL acknowledges the support the Camille and Henry Dreyfus Foundation through their support as a Camille Dreyfus Teacher Scholar.

RSP acknowledges the support the B.P. Faculty Fellowship in the Swanson School of Engineering at the University of Pittsburgh.

References

[1] Sam N. Rothstein, William J. Federspiel, Steven R. Little, A simple model framework for the prediction of controlled release from bulk eroding polymer matrices, J. Mater. Chem. 18 (16) (2008) 1873–1880.
[2] Sam N. Rothstein, William J. Federspiel, Steven R. Little, A unified mathematical model for the prediction of controlled release from surface and bulk eroding polymer matrices, Biomaterials 30 (8) (Mar 2009) 1657–1664.
[3] Sam N. Rothstein, Steven R. Little, A tool box for rational design of degradable controlled release formulations, J. Mater. Chem. 21 (1) (2011) 29–39.
[4] Juergen Siepmann, et al., Effect of the size of biodegradable microparticles on drug release: experiment and theory, J. Control. Release 96 (1) (Apr 2004) 123–134.
[5] Juergen Siepmann, et al., How autocatalysis accelerates drug release from PLGA-based microparticles: a quantitative treatment, Biomacromolecules 6 (4) (2005) 2312–2319.
[6] Gesine Schliecker, et al., Hydrolytic degradation of poly(lactide-co-glycolide) films: effect of oligomers on degradation rate and crystallinity, Int. J. Pharm. 266 (1–2) (Nov 2003) 39–49.
[7] Xin-Hua Zong, et al., Structure and morphology changes in absorbable poly(glycolide) and poly(glycolide- co -lactide) during in vitro degradation, Macromolecules 32 (24) (Nov 1999) 8107–8114.
[8] Minna Hakkarainen, Ann-christine Albertsson, Sigbritt Karlsson, Weight losses and molecular weight changes correlated with the evolution of hydroxyacids in simulated in vivo degradation of homo- and copolymers of PLA and PGA, Polym. Degrad. Stab. 52 (3) (Jun 1996) 283–291.
[9] William E. Schiesser, Graham W. Griffiths, A Compendium of Partial Differential Equation Models: Method of Lines Analysis with Matlab, 1st editionCambridge University Press, Cambridge, Mar 16 2009 (490 pp.).
[10] Fengying Sun, et al., Studies on the preparation, characterization and pharmacological evaluation of tolterodine PLGA microspheres, Int. J. Pharm. 397 (1–2) (Sept 2010) 44–49.
[11] James Thewlis, Concise dictionary of physics and related subjects, Pergamon Press, 1973. (386 pp.).
[12] Andreas M. Sophocleous, et al., The nature of peptide interactions with acid end-group PLGAs and facile aqueous-based microencapsulation of therapeutic peptides, J. Control. Release 172 (3) (Dec 2013) 662–670.
[13] N. Bölgen, et al., In vitro and in vivo degradation of non-woven materials made of poly(epsilon-caprolactone) nanofibers prepared by electrospinning under different conditions, J. Biomater. Sci. Polym. Ed. 16 (12) (Jan 2005) 1537–1555.
[14] Da-Feng Chu, et al., Pharmacokinetics and in vitro and in vivo correlation of huperzine A loaded poly(lactic-co-glycolic acid) microspheres in dogs, Int. J. Pharm. 325 (1–2) (Nov 2006) 116–123.
[15] Jack R. Frautschi, et al., Degradation of polyurethanes in vitro and in vitro: comparison of different models, Colloids Surf. B: Biointerfaces 1 (5) (Nov 1993) 305–313.
[16] Yihong Gong, et al., In vitro and in vivo degradability and cytocompatibility of poly(l-lactic acid) scaffold fabricated by a gelatin particle leaching method, Acta Biomater. 3 (4) (Jul 2007) 531–540.
[17] Christopher, X.F. Lam, et al., Dynamics of in vitro polymer degradation of polycaprolactone-based scaffolds: accelerated versus simulated physiological conditions, Biomed. Mater. (Bristol, Engl.) 3 (3) (Sept 2008) (034108-034108).
[18] P. Taddei, P. Monti, R. Simoni, Vibrational and thermal study on the in vitro and in vivo degradation of a bioabsorbable periodontal membrane: vicryl periodontal mesh (Polyglactin 910), J. Mater. Sci. Mater. Med. 13 (1) (Jan 2002) 59–64.
[19] M.A. Tracy, et al., Factors affecting the degradation rate of poly(lactide-co-glycolide) microspheres in vivo and in vitro, Biomaterials 20 (11) (Jun 1999) 1057–1062.
[20] N.A. Weir, et al., Degradation of poly-L-lactide. Part 1: in vitro and in vivo physiological temperature degradation, Proc. Inst. Mech. Eng. H J. Eng. Med. 218 (5) (Jan 2004) 307–319.
[21] Banu S. Zolnik, Diane J. Burgess, Evaluation of in vivo-in vitro release of dexamethasone from PLGA microspheres, J. Control. Release 127 (2) (Apr 2008) 137–145.
[22] Yoshiro Kobayashi, The role of chemokines in neutrophil biology, Front. Biosci. 13 (2008) 2400–2407.
[23] Xiaodun Mou, et al., Modulation of the foreign body reaction for implants in the subcutaneous space: microdialysis probes as localized drug delivery/sampling devices, J. Diabetes Sci. Technol. 5 (3) (May 2011) 619–631.
[24] W. Kenneth Ward, A Review of the Foreign-body Response to Subcutaneously-implanted Devices: A Review of the Foreign-body Response to Subcutaneously-implanted Devices: The Role of Macrophages and Cytokines in Biofouling and Fibrosis, J. Diabetes Sci. Technol. 2 (5) (Sept 1 2008) 768–777.
[25] Nathaniel M. Vacanti, et al., Localized delivery of dexamethasone from electrospun fibers reduces the foreign body response, Biomacromolecules 13 (10) (Oct 2012) 3031–3038.
[26] J.M. Anderson, Biological responses to materials, Annu. Rev. Mater. Res. (2001) 81–110.
[27] J.M. Anderson, A. Rodriguez, D.T. Chang, Foreign body reaction to biomaterials, Semin. Immunol. 20 (2) (2008) 86–100.
[28] J.M. Anderson, M.S. Shive, Biodegradation and biocompatibility of PLA and PLGA microspheres, Adv. Drug Deliv. Rev. 28 (1) (1997) 5–24.
[29] H. Pan, H. Jiang, W. Chen, The biodegradability of electrospun dextran/PLGA scaffold in a fibroblast/macrophage co-culture, Biomaterials 29 (11) (2008) 1583–1592.
[30] Sung Mook Lim, et al., In vitro and in vivo degradation behavior of acetylated chitosan porous beads, J. Biomater. Sci. Polym. Ed. 19 (2008) 453–466.
[31] P. Calvo, J.L. Vila-Jato, M.J. Alonso, Effect of lysozyme on the stability of polyester nanocapsules and nanoparticles: stabilization approaches, Biomaterials 18 (19) (Oct 1997) 1305–1310.
[32] David M. Higgins, et al., Localized immunosuppressive environment in the foreign body response to implanted biomaterials, Am. J. Pathol. 175 (1) (Jul 2009) 161–170.
[33] P.M. Henson, The immunologic release of constituents from neutrophil leukocytes II. Mechanisms of release during phagocytosis and adherence to nonphagocytosable surfaces, J. Immunol. 107 (6) (1971).
[34] I. Ginis, A.I. Tauber, Activation mechanisms of adherent human neutrophils, Blood 76 (6) (Sept 1990) 1233–1239.
[35] S.S. Kaplan, et al., Biomaterial-induced alterations of neutrophil superoxide production, J. Biomed. Mater. Res. 26 (8) (Aug 1 1992) 1039–1051.
[36] S.S. Kaplan, et al., Mechanisms of biomaterial-induced superoxide release by neutrophils, J. Biomed. Mater. Res. 28 (3) (Mar 1994) 377–386.
[37] Wei-Wu Jiang, et al., Phagocyte responses to degradable polymers, J. Biomed. Mater. Res. A 82 (2) (Aug 2007) 492–497.
[38] A.K. McNally, K.M. DeFife, J.M. Anderson, Interleukin-4-induced macrophage fusion is prevented by inhibitors of mannose receptor activity, Am. J. Pathol. 149 (3) (Sept 1996) 975–985.
[39] Joyce Liu, Ursula A. Matulonis, Anti-angiogenic agents in ovarian cancer: dawn of a new era? Curr. Oncol. Rep. 13 (6) (Dec 2011) 450–458.
[40] S.A. Ali, P.J. Doherty, D.F. Williams, Mechanisms of polymer degradation in implantable devices. 2. Poly(DL-lactic acid), J. Biomed. Mater. Res. 27 (11) (Dec 1993) 1409–1418.
[41] K.H. Lee, et al., Hydrolysis of biodegradable polymers by superoxide ions, J. Polym. Sci. A Polym. Chem. 37 (18) (Sept 1999) 3558–3567.
[42] Elizabeth M. Christenson, James M. Anderson, Anne Hiltner, Oxidative mechanisms of poly(carbonate urethane) and poly(ether urethane) biodegradation: in vivo and in vitro correlations, J. Biomed. Mater. Res. A 70 (2) (Aug 2004) 245–255.
[43] K.H. Lee, et al., Why degradable polymers undergo surface erosion or bulk erosion, Biomaterials 23 (21) (Nov 2002) 4221–4231.
[44] H. Benon, J. Bielski, et al., Reactivity of $HO_2/O\text{-}_2$ radicals in aqueous solution, J. Phys. Chem. Ref. Data 14 (Oct 1 1985) 1041–1100.
[45] Jugminder S. Chawla, Mansoor M. Amiji, Biodegradable poly(ε-caprolactone) nanoparticles for tumor-targeted delivery of tamoxifen, Int. J. Pharm. 249 (1–2) (Dec 5 2002) 127–138.
[46] Zhihua Gan, et al., Enzymatic degradation of poly(ε-caprolactone) film in phosphate buffer solution containing lipases, Polym. Degrad. Stab. 56 (2) (May 1997) 209–213.

[47] Darmawan Darwis, et al., Enzymatic degradation of radiation crosslinked poly(caprolactone), Polym. Degrad. Stab. 62 (2) (Nov 1998) 259–265.
[48] Chikara Tsutsumi, et al., The enzymatic degradation of commercial biodegradable polymers by some lipases and chemical degradation of them, Macromol. Symp. 197 (1) (2003) 431–442.
[49] Helena S. Azevedo and Rui L. Reis. "Understanding the Enzymatic Degradation of Biodegradable Polymers and Strategies to Control Their Degradation Rate." In: *Biodegrad. Syst. Tissue Eng. Regen. Med*.
[50] Sven Lindskog, Structure and mechanism of carbonic anhydrase, Pharmacol. Ther. 74 (1) (1997) 1–20.
[51] M.E. Stroppolo, et al., Superefficient enzymes, Cell. Mol. Life Sci. 58 (10) (Sept 1 2001) 1451–1460.
[52] Kimberly A. Hooper, Natalie D. Macon, Joachim Kohn, Comparative histological evaluation of new tyrosine-derived polymers and poly (L-lactic acid) as a function of polymer degradation, J. Biomed. Mater. Res. 41 (3) (1998) 443–454.
[53] Jan W. Leenslag, et al., Resorbable materials of poly(l-lactide): VII. In vivo and in vitro degradation, Biomaterials 8 (4) (Jul 1987) 311–314.
[54] Suming Li, Steve McCarthy, Influence of crystallinity and stereochemistry on the enzymatic degradation of poly(lactide)s, Macromolecules 32 (13) (Jun 1999) 4454–4456.
[55] Suming Li, et al., Enzymatic degradation of polylactide stereocopolymers with predominant d-lactyl contents, Polym. Degrad. Stab. 71 (1) (2000) 61–67.
[56] E.M. Christenson, J.M. Anderson, A. Hiltner, Biodegradation mechanisms of polyurethane elastomers, Corros. Eng. Sci. Technol. 42 (4) (Dec 2007) 312–323.
[57] E.M. Christenson, J.M. Anderson, A. Hiltner, Antioxidant inhibition of poly(carbonate urethane) in vivo biodegradation, J. Biomed. Mater. Res. A 76A (3) (2006) 480–490.